ACS APPLIED MATERIALS & INTERFACES

Research Article

www.acsami.org

Multi-3,3′-Bicarbazole-Substituted Arylsilane Host Materials with Balanced Charge Transport for Highly Efficient Solution-Processed Blue Phosphorescent Organic Light-Emitting Diodes

Dianming Sun,[†] Xiaokang Zhou,[‡] Huihui Li,[†] Xiaoli Sun,[†] Zhongjie Ren,*[,†] Dongge Ma,[‡] and Shouke Yan*[,†]

[†]State Key Laboratory of Chemical Resource Engineering, Beijing University of Chemical Technology, Beijing 100029, China

[‡]State Key Laboratory of Polymer Physics and Chemistry, Changchun Institute of Applied Chemistry, Chinese Academy of Sciences, Changchun 130022, China

Supporting Information

ABSTRACT: A series of 3,3′-bicarbazole (mCP)-functionalized tetraphenylsilane derivatives (SimCP*x*), including bis(3,5-di(9*H*-carbazol-9-yl)phenyl)diphenylsilane (SimCP2), tris(3,5-di(9*H*-carbazol-9-yl)phenyl)methylsilane (SimCP3-CH_3), tris-(3,5-di(9*H*-carbazol-9-yl)phenyl)phenylsilane (SimCP3-Ph), and tetrakis(3,5-di(9*H*-carbazol-9-yl)phenyl)silane (SimCP4), serving as bipolar blue hosts for bis[2-(4,6-difluorophenyl)pyridyl-*N*,C2′]iridium(III) (FIrpic), have been synthesized by incorporating different ratios of mCP subunits into a central silicon atom. All of the SimCP*x* derivatives have wide bandgaps and high triplet energies because of the indirect linkage by silicon between each mCP subunit. The good solubility and high thermal and morphological stability of SimCP*x* are beneficial for forming amorphous and homogeneous films through solution processing. Density functional theory simulations manifest the better bipolar characteristics for SimCP*x* using three and four mCP units rather than the represented bipolar host SimCP2. As a result, SimCP4 presents the best electron-transporting ability for charge balance. Consequently, the lowest driving voltage of 4.8 eV, and the favorable maximum efficiencies of 14.2% for external quantum efficiency (28.4 cd A^{-1}, 13.5 lm W^{-1}), are achieved by solution-processed, SimCP4-based blue phosphorescent organic light-emitting diodes as the highest performance among SimCP*x*, in which 32% improved device efficiencies compared to that of SimCP2 are obtained. It is inspiring to develop efficient bipolar hosts for blue phosphors by just incorporating monopolar carbazole into arylsilanes in two steps.

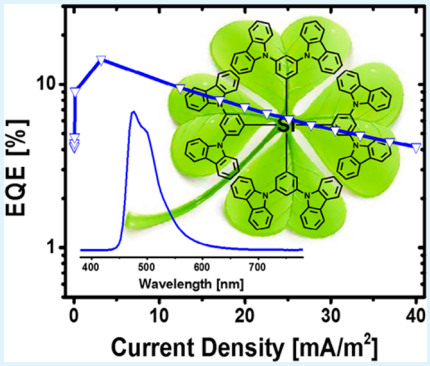

KEYWORDS: *blue phosphorescent OLEDs, small molecule host materials, carbazole, tetraphenylsilane, bipolar host*

INTRODUCTION

With the rapid development of phosphorescent organic light-emitting diodes (PhOLEDs) for realizing flexible displays and solid-state lighting applications, proper host materials are becoming vital to suppress emitter self-quenching and triplet−triplet annihilation for realizing high performance, especially the hosts for blue PhOLEDs with high triplet energies.[1−21] It is important for an ideal host to possess good bipolar transport properties to balance holes and electrons and to achieve higher triplet energy (E_T) (>2.7 eV for bis[2-(4,6-difluorophenyl)pyridyl-N,C2′]iridium(III) (FIrpic)) than the dopant materials to ensure triplet excitons confined in the emitting layer, especially for blue PhOLEDs.[22,23] In addition, the host should be stable upon heating and form good quality films to prolong device life.[24]

To date, a number of blue PhOLEDs with high quantum efficiencies have been realized by vacuum thermal deposition, but high fabrication cost, processing complexity, and poor reproducibility still hinder the practical application of large area blue devices. In contrast, spin-coating and inkjet printing as the wet-processing techniques have been promising methods for realizing simple device configurations, which are desirable for large-area and flexible displays.[25,26] Generally, polymers are suitable to form large-size excellent amorphous films via solution-based deposition techniques at much lower costs.[27] However, the lower purity than that of small molecules limits their display lifetime and efficiency. Our interests focus on combining the advantages of both small molecules and polymers to develop an ideal host for solution-processed blue PhOLEDs. However, achieving this goal has remained a challenge. On the one hand, most small molecule hosts are easy to crystallize due to their small molecule size. On the other hand, for bipolar properties to be realized, efficient electron-transporting moieties are often incorporated into the hosts to enhance electrical properties. Nevertheless, it is noteworthy that there have not been many applicable electron deficient units for high triplet energy hosts; meanwhile, further extended molecular systems with more subunits and complicated linkages

Received: May 12, 2015
Accepted: August 3, 2015
Published: August 7, 2015

DOI: 10.1021/acsami.5b04112
ACS Appl. Mater. Interfaces 2015, 7, 17802−17810

Scheme 1. Synthetic Procedure for SimCP*x*

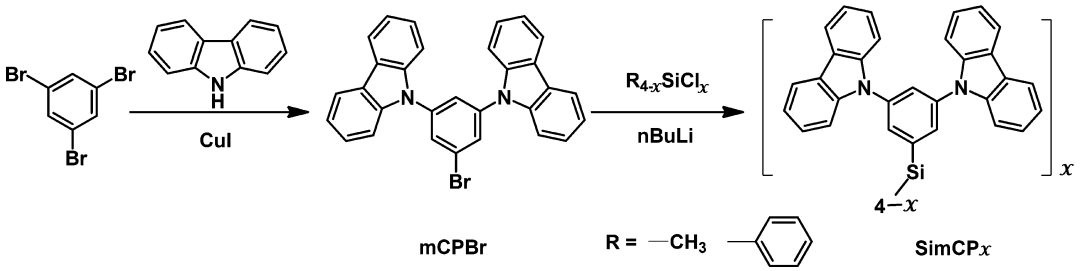

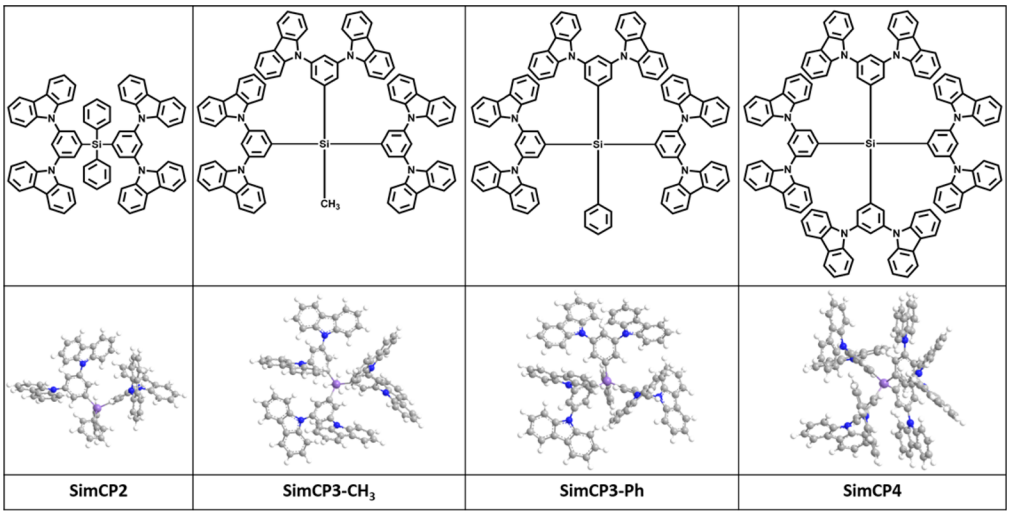

Figure 1. Molecular structures and stereographs of optimized tetraphenylsilane-core-based oligomers SimCP*x* at the B3LYP/6-31G(d) level.

will inevitably raise production cost. Therefore, there is a demand for designing bipolar hosts with high triplet energies and easily produced structures for blue phosphorescence emitters.

Among most functional segments for ideal host materials, carbazole has been widely chosen because of its distinct properties, such as high triplet energy, good solubility, and facile functionalization.[28−33] However, it is difficult to obtain bipolar transport abilities by just using carbazole subunits due to their strong hole transport character. A representative bipolar host, bis(3,5-di(9H-carbazol-9-yl)phenyl)diphenylsilane (SimCP2) with a carbazole moiety as the only functional group, was developed by Chen's group.[34] Different from most small molecule hosts with highly crystallinity and low thermal stability in the solid state, SimCP2 is completely amorphous and can form highly stable thin films. Importantly, it preserves the characteristics of adequate high electron and hole-carrier mobilities of ~10^{-4} cm^2 V^{-1} s^{-1} and a sufficiently high triplet state energy of ~3.01 eV in confining emission energy on FIrpic. Recently, spectroscopic comparsion between 3,5-di(*N*-carbazolyl)tetraphenylsilane (SimCP) and SimCP2 has revealed that the intersystem crossing rate for SimCP2 was smaller than for SimCP, leading to a higher energy transfer rate from SimCP2 to FIrpic than from SimCP. Thus, it is possible to improve the performance of SimCP2 with increasing mCP subunits. Herein, a systematic study of SimCP2 analogues with more than two mCP functionalized silanes was carried out, and the relationship between the different ratios of functional subunits to the silicon atom and photophysical properties of device performances has also been presented.

In this contribution, a series of SimCP2 analogues based on the tetraphenylsilane-core structure functionalized with different ratios of mCP subunits for the collective name SimCP*x*, namely, bis(3,5-di(9*H*-carbazol-9-yl)phenyl)diphenylsilane (SimCP2), tris(3,5-di(9*H*-carbazol-9-yl)phenyl)methylsilane (SimCP3-CH_3), tris(3,5-di(9*H*-carbazol-9-yl)phenyl)-phenylsilane (SimCP3-Ph), and tetrakis(3,5-di(9*H*-carbazol-9-yl)phenyl)silane (SimCP4), have been designed and synthesized as high triplet energy hosts for blue PhOLEDs. As a result, the blue PhOLED hosted by SimCP4 exhibited the highest performance among the SimCP*x*-based devices, including a high current efficiency of 28.4 cd A^{-1} and an external quantum efficiency (EQE) of 14.2% with Commission International de l'Eclairage (CIE) coordinates of (0.156, 0.355). The high maximum efficiencies are among the best solution-processed blue PhOLEDs reported in the literature.[19,32] This work not only demonstrates a series of highly efficient blue electrophosphorescent bipolar hosts but also determines the influences of molecular structures on electroluminescence performance, which originates from its contributions in charge transport balance and film forming stability.

RESULTS AND DISCUSSION

Synthesis and Characterization. The synthetic route and chemical structures of SimCP2, SimCP3-CH_3, SimCP3-Ph, and SimCP4 are shown in Scheme 1 and Figure 1. SimCP*x* can be easily synthesized in two steps, first by copper-catalyzed Ullman coupling of 1,3,5-tribromobenzene with two equiv of carbazole, followed by a lithium exchange reaction with silane chloride in excellent yield. Their molecular structures were confirmed by NMR spectroscopy (see Supporting Information) and

DOI: 10.1021/acsami.5b04112
ACS Appl. Mater. Interfaces 2015, 7, 17802−17810

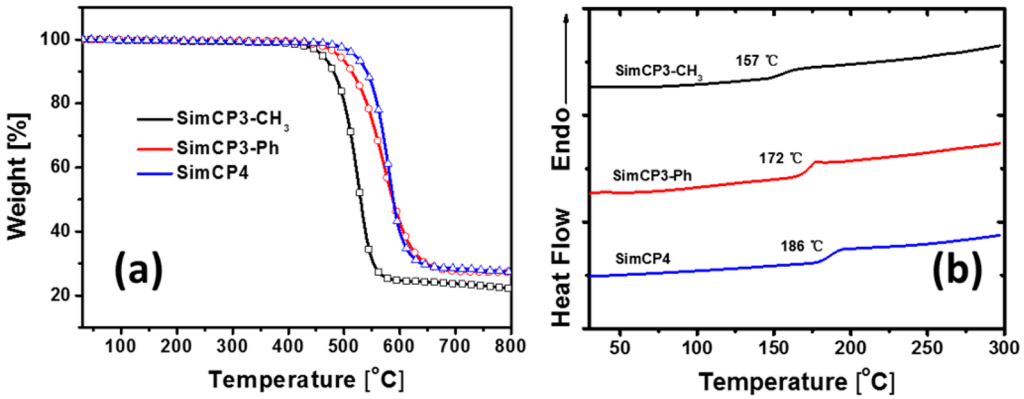

Figure 2. (a) TGA traces of SimCP*x* recorded at a heating rate of 10 °C min^{-1}. (b) DSC measurements recorded at a heating rate of 10 °C min^{-1}.

elemental analyses. All compounds show good solubility. They are easily soluble in common organic solvents, such as chloroform, tetrahydrofuran, toluene, and chlorobenzene.

Thermal Properties. To determine the thermal properties of SimCP3-CH$_3$, SimCP3-Ph, and SimCP4, thermogravimetric analysis (TGA) and differential scanning calorimetry (DSC) analyses were performed under a nitrogen atmosphere at a heating rate of 10 °C min^{-1} (Figure 2 and Table 1). It was shown that the temperature of decomposition (T_d) remarkably increased from 461 to 490 to 519 °C with enlarging molecular weight, which should be the combined result of reduced volatility and enhanced molecular rigidity for SimCP3-CH$_3$, SimCP3-Ph, and SimCP4, respectively, with the higher molecular weight and more bulky groups. Accordingly, their glass transition temperatures (T_g) determined by DSC revealed the same order from 157 to 172 to 186 °C for SimCP3-CH$_3$, SimCP3-Ph, and SimCP4, respectively (Figure 2b). These values are outstanding among small molecules, which are significantly higher than that of the corresponding mCP bulky group (T_g = 60 °C) and the commonly used host material SimCP2 (T_g = 144 °C). For SimCP2, the physical properties are listed in Table 1 according to previously published work.[35]

Table 1. Thermal, Photophysical, and Electrochemical Data of SimCP*x*

compound	T_g[a] (°C)	T_d[b] (°C)	λ_{abs}[c] (nm)	$\lambda_{em,max}$[d] (nm)	HOMO[e] (eV)	LUMO[f] (eV)
SimCP2	144	466	348	344, 360, 378	−5.65	−2.08
SimCP3-CH3	157	461	346	346, 361, 380	−5.66	−2.08
SimCP3-Ph	172	490	346	346, 361, 380	−5.69	−2.11
SimCP4	186	519	346	345, 360, 380	−5.65	−2.07

[a]Obtained from DSC measurements. [b]Obtained from TGA measurements. [c]Measured in dichloromethane. [d]Measured in PS films doped with 3 wt % SimCP*x*. [e]Determined from the onset of oxidation potentials. [f]Deduced from HOMO and E_g estimated from the red edge of the longest absorption wavelength for the solid-film sample.

Morphological Properties. The film-forming ability of SimCP*x* and miscibility to the dopant FIrpic were also investigated by atomic force microscopy (AFM). As shown in Figure 3, the AFM image of 10 wt % FIrpic-doped SimCP*x* films displays fairly smooth and homogeneous morphology with small values of root-mean-square (RMS) roughness of 0.46, 0.43, and 0.51 nm for SimCP3-CH$_3$, SimCP3-Ph, and SimCP4, respectively. It is free of particle aggregation or phase separation, suggesting good film forming ability and good miscibility of FIrpic.

Photophysical Properties. The photophysical properties of SimCP*x* were investigated by their ultraviolet−visible (UV−vis) absorption and low-temperature photoluminance (PL) spectra (Figure 4a). The photophysical data of these compounds are summarized in Table 1. The profiles of absorption spectra in dilute dichloromethane solution are similar from 240 to 360 nm with three main absorption bands. The peaks at ∼293 nm are assigned to $\pi \rightarrow \pi^*$ transitions of the carbazole moiety, and the weaker absorption peaks at the longer wavelengths of 326 and 340 nm could be attributed to the n $\rightarrow \pi^*$ transitions of extended conjugation of the carbazole moiety. Estimated from their absorption edges, the energy gap (E_g) of SimCP*x* is ∼3.58 eV with negligible discrepancies <0.01 eV.

The analogical PL spectra among SimCP3-CH$_3$, SimCP3-Ph, and SimCP4 are compared in Figure 4b, where the spectra are normalized at the most intense S_1 emission peak. The fluorescent spectra of 3 wt % SimCP*x* doped in PS thin films are almost identical. The short-wavelength region is composed

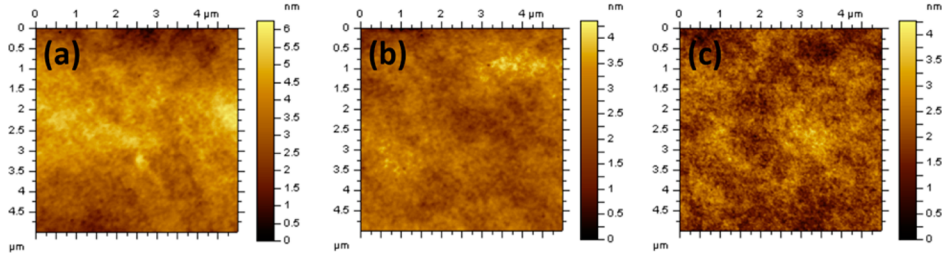

Figure 3. AFM topographical images of the solution-processed films of SimCP*x* doped with 10 wt % FIrpic: (a) SimCP3-CH$_3$, (b) SimCP3-Ph, and (c) SimCP4.

DOI: 10.1021/acsami.5b04112
ACS Appl. Mater. Interfaces 2015, 7, 17802−17810

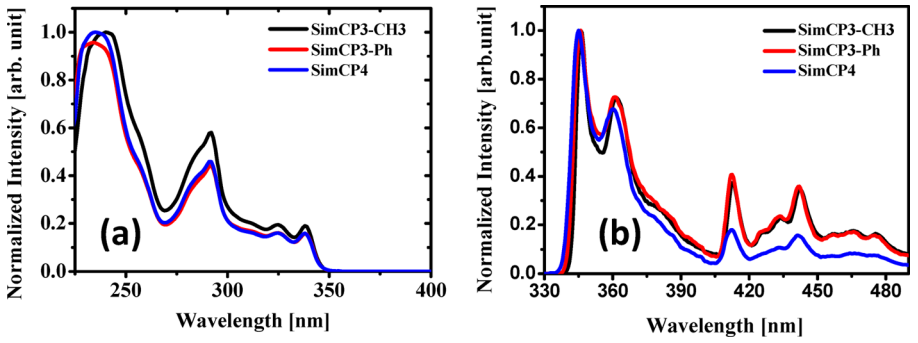

Figure 4. (a) Absorption spectra of SimCP*x* in dichloromethane measured at room temperature (10^{-6} mol L^{-1}). (b) Low-temperature (77 K) emission spectra of PS thin films doped with 3 wt % SimCP*x*. Absorption spectra are cut at $\lambda < 240$ nm for the solution case because of strong absorption of the solvent.

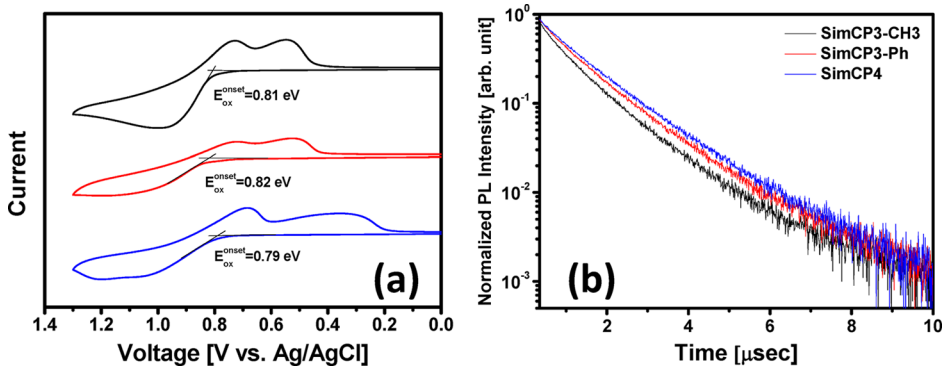

Figure 5. (a) Cyclic voltammograms of SimCP3-CH_3, SimCP3-Ph, and SimCP4 in CH_2Cl_2 for an oxidation scan. (b) Transient photoluminescence decay (excited at 343 nm) curves at 475 nm for SimCP3-CH_3, SimCP3-Ph, and SimCP4 doped with 10 wt % of FIrpic.

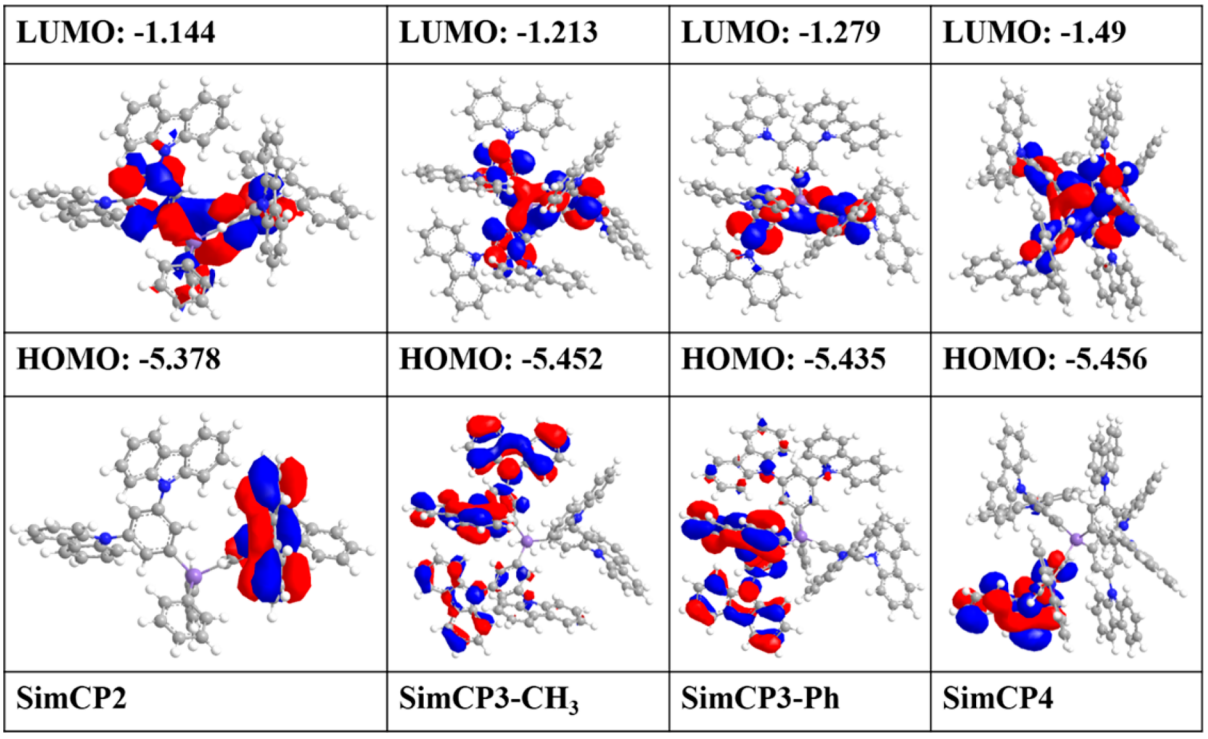

Figure 6. Frontier molecular orbitals of SimCP2, SimCP3-CH_3, SimCP3-Ph, and SimCP4.

of three bands, including a main peak at ~345 nm and two shoulder peaks at approximately 360 and 380 nm, which originate from the lowest vibrational state of the first excited singlet state to the three lowest vibrational states of the ground state, respectively. Similarly, in the phosphorescence region, four weak PL bands at 412, 425, 433, and 442 nm are attributed

DOI: 10.1021/acsami.5b04112
ACS Appl. Mater. Interfaces 2015, 7, 17802−17810

to the transition from the T_1 state. Taking into account that SimCP3-CH_3, SimCP3-Ph, and SimCP4 consist of three or four mCP molecules, their S_1 and T_1 electronic states are determined mainly by the mCP molecule. However, the intensity ratios of the one-phonon S_1 emission peak to the most intense zero-phonon S_1 emission peak vary slightly with 0.723, 0.726, and 0.676 for SimCP3-CH_3, SimCP3-Ph, and SimCP4, respectively. It becomes small with decreased distance between the equilibrium position of the first excited singlet state and the equilibrium position of the ground state, which indicates the electron−phonon coupling between the first excited singlet state and ground state for SimCP4 is slightly smaller than that of SimCP3-CH_3 and SimCP3-Ph, as shown in Figure 4.

Another intensity ratio of the zero-phonon band intensity of the T_1 emission to that of the S_1 emission can be used to speculate the strength of spin−orbit coupling. The smaller the ratio, the weaker is the strength of spin−orbit coupling. From the ratio, it can be deduced that the strength of spin−orbit coupling for SimCP4 is weaker than for SimCP3-CH_3 and SimCP3-Ph. The weakest spin−orbit coupling of SimCP4 reduces the intersystem crossing rate (ISC) from the excited singlet states to the triplet states. As for the FIrpic/SimCP*x* doping system, the singlet energy will transfer from the wide bandgap host via the Förster process to the singlet state of FIrpic. Furthermore, the low ISC rate of the SimCP4 host will lead to a high energy transfer rate to the dopant. Therefore, higher device efficiencies for SimCP4 can be expected.

Electrochemical Properties. The electrochemical behaviors of these compounds were tested by cyclic voltammetry in anhydrous dichloromethane under a nitrogen atmosphere (Figure 5a). All of the $SimCP_X$ analogues exhibit an irreversible oxidation feature as those of other carbazole derivatives with unprotected 3,6-positions. The oxidation onset potentials versus Ag/Ag^+ were recorded at 0.81, 0.82, and 0.79 V for SimCP3-CH_3, SimCP3-Ph, and SimCP4, respectively. According to the empirical formula $E_{HOMO} = -(4.8 + E_{ox}^{on} - E_{Fc})$ eV, the HOMO energy levels of SimCP*x* were calculated as shown in Table 1, which is consistent with the molecular simulation shown in Figure 6. The HOMO level with negligible differences within 0.03 eV confirmed the approximate electroactivity of SimCP*x*, and their HOMO levels match well with that of the hole-injecting material poly(3,4-ethylenedioxythiopene):poly-(styrenesulfonate) (PEDOT:PSS) (−5.20 eV), which would result in an efficient hole-injection from PEDOT:PSS to the emissive layer. The LUMO energy level could be calculated by adding the optical E_g to the HOMO level (Table 1). Their LUMOs were found to be higher than those of conventional phosphorescence emitters, especially blue-emitting FIrpic (−2.7 eV) (Figure 7), leading to predominant direct charge recombination on phosphorescent dopants for realizing high EL efficiencies.

We also performed transient photoluminescence measurements to verify the exciton confinement property of these hosts at a wavelength of 475 nm for SimCP*x* films doped with 10 wt % of FIrpic on quartz substrates. Figure 5b shows almost identical monoexponential decay curves, indicating that the triplet energy transfer from FIrpic to SimCP*x* is completely suppressed and that the energy is effectively confined in the emission layer.

Frontier Molecular Orbitals Simulation. The lowest unoccupied molecular orbital (LUMO) and the highest occupied molecular orbital (HOMO) wave functions of SimCP*x* are depicted in Figure 6. As expected, the HOMO

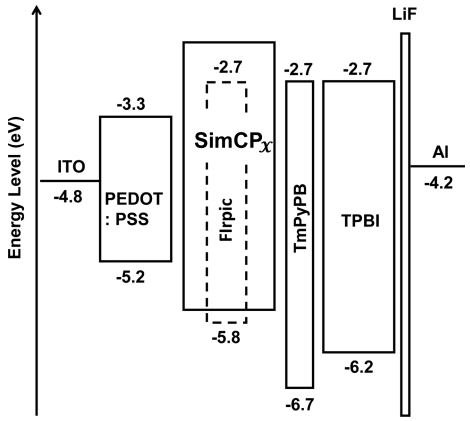

Figure 7. Energy level diagram for the SimCP*x*-based devices.

wave functions are delocalized mainly on the carbazole subunits with small contributions from the phenyl substituents on the carbazole N atoms. In contrast, the LUMO wave functions reside on the phenyl bridge linked to the central silicon atom. This result indicates that the spatial weak overlap between the HOMO and LUMO may result in weaker optical absorption corresponding to the transition from HOMO to LUMO. In addition, the differences between energy levels of LUMOs or HOMOs for SimCP*x* are no more than 0.1 eV, except for SimCP4 with more shadow LUMO. It is expected that the lower LUMO will improve the electron-injecting ability. Furthermore, as the number of mCP subunits increase, the LUMOs simultaneously decrease, which is accompanied by an improved ability to inject electrons from an adjacent electron-transporting layer. Consequently, SimCP4 has the smallest HOMO−LUMO gap (Δ_{H-L}), which is not consistent with the CV results above. Here, our calculated energy gap Δ_{H-L} in theory is the orbital energy difference between HOMO and LUMO. Experimentally, it can almost be obtained from the absorption spectra, which is the lowest excitation energy from ground state S_0 to excited state S_1, termed the optical band gap (E_g). In fact, the optical band gap is not the orbital energy difference between HOMO and LUMO, but the energy difference between the S_0 and S_1 states. The values of the optical band gap may equal the HOMO−LUMO gap only when the excitation from the S_0 to S_1 state corresponds almost exclusively to the electron transition from the HOMO to the LUMO.

These results indicate that the HOMO, LUMO, and Δ_{H-L} of SimCP*x* are affected by the number of introduced mCP subunits. As shown in Figure 6, the carbazole units are significantly twisted, resulting in a nonplanar structure in each molecule. These geometrical characteristics can effectively suppress molecular recrystallization and thus improve the morphological stability of the thin film and keep the triplet energy gap at a high level.

Reorganization Energy. The calculated reorganization energies for holes (λ_h) and electrons (λ_e) are listed in Table 2. It is well established that lower reorganization energy values will result in higher charge transfer rates. It is clearly seen that the calculated λ_e value of SimCP4 is the smallest among all of the SimCP*x* derivatives. For SimCP3-CH_3, SimCP3-Ph, and SimCP4, the λ_h values are almost identical. Moreover, the λ_e values are all lower than that of SimCP2, and the sequence of λ_e values is SimCP2 > SimCP3-CH_3 > SimCP3-Ph > SimCP4. Generally, the holes are dominantly the majority carrier in most

DOI: 10.1021/acsami.5b04112
ACS Appl. Mater. Interfaces 2015, 7, 17802−17810

Table 2. Calculated Reorganization Energies for Electrons (λ_e) and Holes (λ_h) of the Molecules for SimCP*x* at the B3LYP/6-31G(d) Level

species	λ_h (eV)	λ_e (eV)
SimCP2	0.0411	0.315
SimCP3-CH_3	0.0514	0.299
SimCP3-Ph	0.0499	0.290
SimCP4	0.0507	0.253

conventional devices. Therefore, the improved electron-transporting ability would balance charge carrier injection and promote exciton recombination in emitting layers (EML). It suggests that SimCP4 with the smallest λ_e value could be a better bipolar host than the representative bipolar SimCP2. Furthermore, we find that reorganization energy λ_e correlates well with the change of geometry upon ionization. The smaller changes correspond to the smaller values of λ_e. It can be seen from Figure 6 that the volume steric hindrance of SimCP*x* improves along with the increased mCP subunits, which decrease geometry changes and lower the values of λ_e.

The bipolar properties of SimCP2, SimCP3-CH3, SimCP3-Ph, and SimCP4 were confirmed by hole-only and electron-only devices. The structure for hole-only devices was ITO/PEDOT:PSS/hosts (60 nm)/Al, and the structure for electron-only devices was ITO/hosts (60 nm)/TPBi (30 nm)/LiF (1 nm)/Al. As seen in Figure S1, the current density−voltage curves of hole- and electron-only devices indicate bipolar charge transport properties of SimCP2, SimCP3-CH3, SimCP3-Ph, and SimCP4. Moreover, the maximum electron current density of SimCP4 matches well with the result of calculated electron reorganization energy. As the carbazole units increases, the electron-transporting ability improved significantly for these tetraphenylsilane derivatives, thus balancing holes and electrons in the emitting layer.

Electroluminescent Performance of Blue PHOLEDs. To examine the influence of energy levels and reorganization energies on device efficiency, we fabricated a series of blue-emitting PhOLEDs based on SimCP3-CH_3, SimCP3-Ph, and SimCP4 by spin-coating as devices **B**, **C**, and **D** with the device configuration of ITO/PEDOT:PSS/SimCP*x*:FIrpic (50 nm, 10%)/Tm3PyPB (5 nm)/TPBi (30 nm)/LiF/Al, where PEDOT:PSS and LiF serve as hole- and electron-injecting layers, and TPBi serves as the electron-transporting layer; Tm3PyPB[36] was used as the hole/exciton-blocking layer, and SimCP*x* doped with 10 wt % of FIrpic was spin-coated to form an emitting layer (Figure 7). Control device **A**, based on conventional host SimCP2, was also fabricated with the same configuration. We focus on investigating the structural effects of SimCP*x* on device performance, and the conventional device structure was employed without any further optimization.

Panels a−d in Figure 8 depict the current density−voltage, brightness−voltage characteristics, and device efficiencies. Table 3 summarizes the electroluminescence (EL) data obtained and compares it to the data from the literature with the same configuration. The blue devices possess relatively low turn-on voltages (4.8−5.4 eV), which decrease gradually from device **A** to **D**. The decrease in turn-on voltage can be attributed to the dropping calculated LUMOs and reorganization of λ_e as validated by DFT simulation. Meanwhile, it may help to reduce the electron injection barrier and improve electron mobility in the devices, and thus, the charge flux in device **D** tends to be more balanced relative to that of devices **A**−**C**. In addition, the best EL performance was achieved for SimCP4-based device **D** with CE_{max} of 28.42 cd A^{-1}, PE_{max} of 13.52 lm W^{-1}, and EQE_{max} of 14.2%. Devices **B** and **C**, with

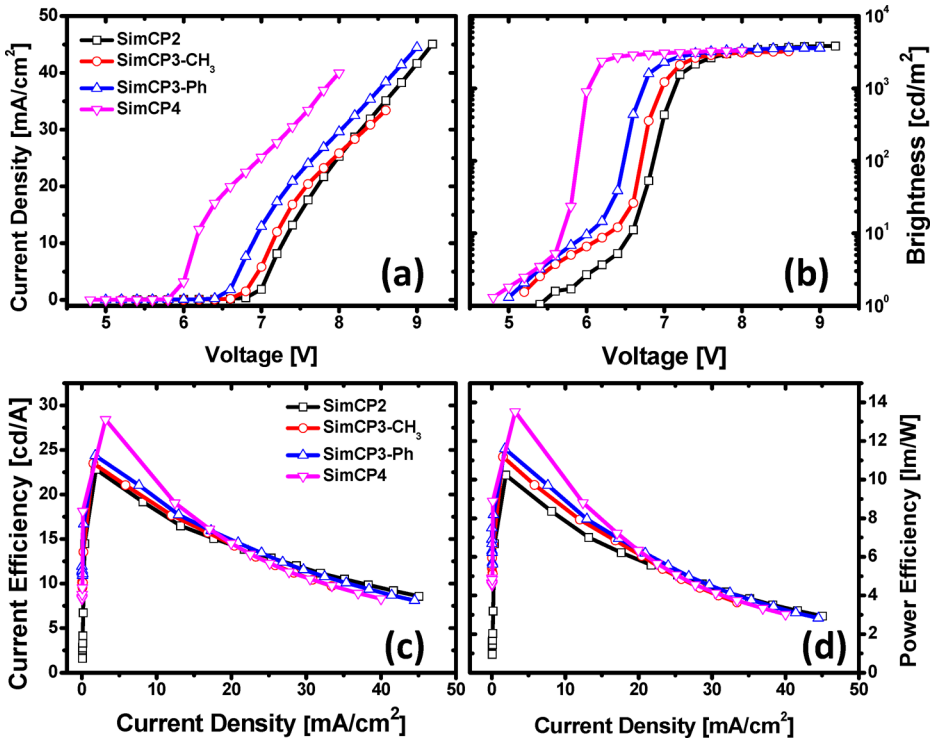

Figure 8. (a) *J*−*V* curves, (b) *L*−*V* curves, (c) current efficiency versus current density curves, and (d) power efficiency versus current density of FIrpic-doped devices **A**−**D** (see Table 3).

DOI: 10.1021/acsami.5b04112
ACS Appl. Mater. Interfaces 2015, 7, 17802−17810

Table 3. Performances of FIrpic-Based, Solution-Processed Devices with the Configuration of ITO/PEDOT:PSS/host:FIrpic/Tm3PyPB (5 nm)/TPBi (30 nm)/LiF or CsF/Al

	V_{on} (V)[a]	L_{max} (cd/m^2)[b]	$\eta_{c,max}$ (cd/A)[c]	$\eta_{p,max}$ (lm/W)[d]	$\eta_{ext,max}$ (100%)[e]	CIE (x, y)[f]
PCzMSi[18]	5.5	7299	22.8	9.4	11.9	0.15, 0.33
PCzPhSi[18]	5.1	6532	20.7	8.3	11.0	0.15, 0.33
CSPO[19]	7.8	333	1.49	0.51	0.58	0.17, 0.34
DCSPO[19]	7.6	6245	6.27	2.07	3.1	0.16, 0.33
CS_2PO[19]	8.0	2241	20.17	7.37	10.4	0.16, 0.33
DCS_2PO[19]	8.6	4878	26.5	8.66	13.6	0.15, 0.33
PDCzMSi[37]	5.0	4730	17.7	7.7	9.2	0.15, 0.33
PCzSiPh[38]	5.8	12421	29.3	10.4	14.3	0.15, 0.32
PmCPSi[39]	5.8	6930	18.93	6.32	9.2	0.15, 0.33
A SimCP2	5.4	3869	22.83	10.24	10.8	0.178, 0.382
B SimCP3-CH_3	5.2	3252	23.49	11.18	11.2	0.171, 0.377
C SimCP3-Ph	5.0	3606	24.38	11.6	12.0	0.155, 0.364
D SimCP4	4.8	3319	28.42	13.52	14.2	0.156, 0.355

[a]Turn-on voltage recorded at a brightness of 1 cd m^{-2}. [b]Maximum luminance. [c]Maximum current efficiency. [d]Maximum power efficiency. [e]Maximum external quantum efficiency. [f]Commission International de l'Eclairage (CIE) coordinates at the turn-on voltage.

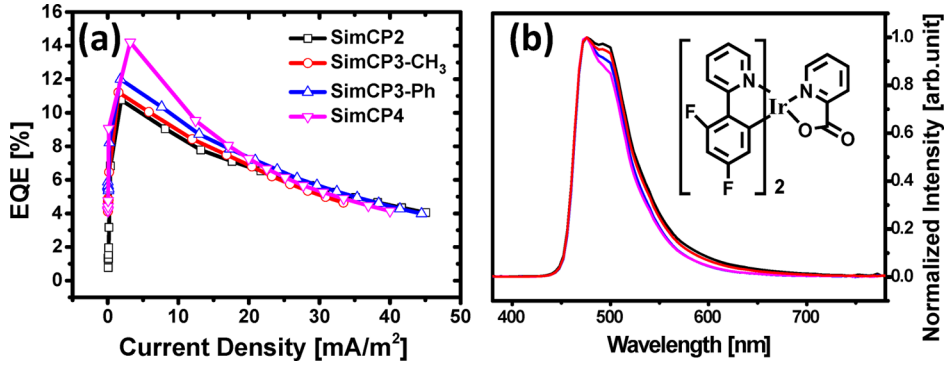

Figure 9. (a) External quantum efficiency versus current density and (b) electroluminance spectra for FIrpic-doped devices **A**–**D**.

three mCP units, exhibited almost approximate performances, which were slightly better than that of device **A**. These values indicate that spin-coated SimCP*x*:FIrpic-based devices are comparable to the highest values reported for solution-processed, FIrpic-based devices and could even compete with more complicated device architectures.

The normalized electroluminance spectra of devices **A**–**D** are shown in Figure 9b, and the Commission International de l'Eclairage (CIE) coordinates are listed in Table 3. As can clearly be seen, all of the spectra show the same main emission peak at 472 nm, corresponding to the emission of FIrpic, and their EL bands are nearly identical. Hence, the EL originates only from the FIrpic molecule, indicating an essentially complete energy or charge transfer from the hosts to FIrpic, which is consistent with the PL spectra, as shown in Figure S2. It was noticeable that, from device **A** to **D**, the vibronic shoulder emission peak of FIrpic was effectively suppressed in EL spectra owing to the nonpolar environment provided by SimCP4, resulting in the improved color purities. Therefore, for devices **A**–**D**, an obvious CIE change can be seen from (0.178, 0.382) for SimCP2 to (0.156, 0.355) for SimCP4, which confirms that SimCP4 is a better host than SimCP2.

CONCLUSIONS

In summary, we have synthesized a series of high triplet energy mCP-functionalized tetraphenylsilane derivatives that can serve as bipolar blue hosts for FIrpic by incorporating different ratios of mCP subunits into a central silicon atom. These analogues exhibit distinct physical properties of good solubility and high thermal and morphological stability, which are beneficial to the formation of amorphous and homogeneous films by solution processing. Density functional theory simulations indicate that SimCP*x* with four mCP subunits shows better electron-transporting ability than the represented bipolar host SimCP2. As a result, the SimCP4-based devices exhibit a lower operational voltage, higher luminance efficiency, improved CIE coordinates, and enhanced EL efficiency compared to those of the SimCP2 device under directly comparable conditions. In particular, it is inspiring to develop efficient bipolar hosts for blue phosphors by just incoporating monopolar carbazole into arylsilanes in two steps.

ASSOCIATED CONTENT

Supporting Information

The Supporting Information is available free of charge on the ACS Publications website at DOI: 10.1021/acsami.5b04112.

Synthetic procedures, characterization methods, device fabrications, and NMR spectra (PDF)

AUTHOR INFORMATION

Corresponding Authors

*E-mail: renzj@mail.buct.edu.cn.
*E-mail: skyan@mail.buct.edu.cn.

Author Contributions

§D.S. and

DOI: 10.1021/acsami.5b04112
ACS Appl. Mater. Interfaces 2015, 7, 17802–17810

X.Z. contributed equally.

Notes

The authors declare no competing financial interest.

■ ACKNOWLEDGMENTS

The financial support of the National Natural Science Foundations of China (Grant No. 21274009 and 51221002) and Beijing Higher Education Young Elite Teacher Project (YETP0491) are gratefully acknowledged.

■ REFERENCES

(1) Tsai, M. H.; Lin, H. W.; Su, H. C.; Ke, T. H.; Wu, C. C.; Fang, F. C.; Liao, Y. L.; Wong, K. T.; Wu, C. I. Highly Efficient Organic Blue Electrophosphorescent Devices Based on 3, 6-Bis (triphenylsilyl) carbazole as the Host Material. *Adv. Mater.* **2006**, *18*, 1216−1220.

(2) Shih, P. I.; Chien, C. H.; Chuang, C. Y.; Shu, C. F.; Yang, C. H.; Chen, J. H.; Chi, Y. Novel Host Material for Highly Efficient Blue Phosphorescent OLEDs. *J. Mater. Chem.* **2007**, *17*, 1692−1698.

(3) Wu, M. F.; Yeh, S. J.; Chen, C. T.; Murayama, H.; Tsuboi, T.; Li, W. S.; Chao, I.; Liu, S. W.; Wang, J. K. The Quest for High-Performance Host Materials for Electrophosphorescent Blue Dopants. *Adv. Funct. Mater.* **2007**, *17*, 1887−1895.

(4) Han, W. S.; Son, H. J.; Wee, K. R.; Min, K. T.; Kwon, S.; Suh, I. H.; Choi, S. H.; Jung, D. H.; Kang, S. O. Silicon-Based Blue Phosphorescence Host Materials: Structure and Photophysical Property Relationship on Methyl/Phenylsilanes Adorned with 4-(N-Carbazolyl) phenyl Groups and Optimization of Their Electroluminescence by Peripheral 4-(N-Carbazolyl) phenyl Numbers. *J. Phys. Chem. C* **2009**, *113*, 19686−19693.

(5) Hsu, F. M.; Chien, C. H.; Shu, C. F.; Lai, C. H.; Hsieh, C. C.; Wang, K. W.; Chou, P. T. A Bipolar Host Material Containing Triphenylamine and Diphenylphosphoryl-Substituted Fluorene Units for Highly Efficient Blue Electrophosphorescence. *Adv. Funct. Mater.* **2009**, *19*, 2834−2843.

(6) Hu, D.; Lu, P.; Wang, C.; Liu, H.; Wang, H.; Wang, Z.; Fei, T.; Gu, X.; Ma, Y. Silane Coupling Di-carbazoles with High Triplet Energy as Host Materials for Highly Efficient Blue Phosphorescent Devices. *J. Mater. Chem.* **2009**, *19*, 6143−6148.

(7) Chou, H. H.; Cheng, C. H. A Highly Efficient Universal Bipolar Host for Blue, Green, and Red Phosphorescent OLEDs. *Adv. Mater.* **2010**, *22*, 2468−2471.

(8) Ding, J.; Wang, Q.; Zhao, L.; Ma, D.; Wang, L.; Jing, X.; Wang, F. Design of Star-Shaped Molecular Architectures Based on Carbazole and Phosphine Oxide Moieties: Towards Amorphous Bipolar Hosts with High Triplet Energy for Efficient Blue Electrophosphorescent Devices. *J. Mater. Chem.* **2010**, *20*, 8126−8133.

(9) Fei, T.; Cheng, G.; Hu, D.; Dong, W.; Lu, P.; Ma, Y. Iridium Complex Grafted to 3, 6-Carbazole-alt-Tetraphenylsilane Copolymers for Blue Electrophosphorescence. *J. Polym. Sci., Part A: Polym. Chem.* **2010**, *48*, 1859−1865.

(10) Cho, Y. J.; Lee, J. Y. Tetraphenylsilane-Based High Triplet Energy Host Materials for Blue Phosphorescent Organic Light-Emitting Diodes. *J. Phys. Chem. C* **2011**, *115*, 10272−10276.

(11) Cho, Y. J.; Lee, J. Y. Low Driving Voltage, High Quantum Efficiency, High Power Efficiency, and Little Efficiency Roll-Off in Red, Green, and Deep-blue Phosphorescent Organic Light-Emitting Diodes Using a High-Triplet-Energy Hole Transport Material. *Adv. Mater.* **2011**, *23*, 4568−4572.

(12) Gong, S.; Fu, Q.; Wang, Q.; Yang, C.; Zhong, C.; Qin, J.; Ma, D. Highly Efficient Deep-Blue Electrophosphorescence Enabled by Solution-Processed Bipolar Tetraarylsilane Host with Both a High Triplet Energy and a High-Lying HOMO Level. *Adv. Mater.* **2011**, *23*, 4956−4959.

(13) Jeon, S. O.; Jang, S. E.; Son, H. S.; Lee, J. Y. External Quantum Efficiency Above 20% in Deep Blue Phosphorescent Organic Light-Emitting Diodes. *Adv. Mater.* **2011**, *23*, 1436−1441.

(14) Bin, J. K.; Cho, N. S.; Hong, J. I. New Host Material for High-Performance Blue Phosphorescent Organic Electroluminescent Devices. *Adv. Mater.* **2012**, *24*, 2911−2915.

(15) Liu, H.; Cheng, G.; Hu, D.; Shen, F.; Lv, Y.; Sun, G.; Yang, B.; Lu, P.; Ma, Y. A Highly Efficient, Blue-Phosphorescent Device Based on a Wide-Bandgap Host/FIrpic: Rational Design of the Carbazole and Phosphine Oxide Moieties on Tetraphenylsilane. *Adv. Funct. Mater.* **2012**, *22*, 2830−2836.

(16) Sasabe, H.; Toyota, N.; Nakanishi, H.; Ishizaka, T.; Pu, Y. J.; Kido, J. 3,3′-Bicarbazole-Based Host Materials for High-Efficiency Blue Phosphorescent OLEDs with Extremely Low Driving Voltage. *Adv. Mater.* **2012**, *24*, 3212−3217.

(17) Fan, C.; Chen, Y.; Liu, Z.; Jiang, Z.; Zhong, C.; Ma, D.; Qin, J.; Yang, C. Tetraphenylsilane Derivatives Spiro-Annulated by Triphenylamine/Carbazole with Enhanced HOMO Energy Levels and Glass Transition Temperatures without Lowering Triplet Energy: Host Materials for Efficient Blue Phosphorescent OLEDs. *J. Mater. Chem. C* **2013**, *1*, 463−469.

(18) Sun, D.; Fu, Q.; Ren, Z.; Li, W.; Li, H.; Ma, D.; Yan, S. Carbazole-Based Polysiloxane Hosts for Highly Efficient Solution-Processed Blue Electrophosphorescent Devices. *J. Mater. Chem. C* **2013**, *1*, 5344−5350.

(19) Liu, H.; Bai, Q.; Yao, L.; Hu, D.; Tang, X.; Shen, F.; Zhang, H.; Gao, Y.; Lu, P.; Yang, B. Solution-Processable Hosts Constructed by Carbazole/PO Substituted Tetraphenylsilanes for Efficient Blue Electrophosphorescent Devices. *Adv. Funct. Mater.* **2014**, *24*, 5881−5888.

(20) Yook, K. S.; Lee, J. Y. Small Molecule Host Materials for Solution Processed Phosphorescent Organic Light-Emitting Diodes. *Adv. Mater.* **2014**, *26*, 4218−4233.

(21) Liu, D.; Du, M.; Chen, D.; Ye, K.; Zhang, Z.; Liu, Y.; Wang, Y. A Novel Tetraphenylsilane-Phenanthroimidazole Hybrid Host Material for Highly Efficient Blue Fluorescent, Green and Red Phosphorescent OLEDs. *J. Mater. Chem. C* **2015**, *3*, 4394−4401.

(22) Chaskar, A.; Chen, H. F.; Wong, K. T. Bipolar Host Materials: A Chemical Approach for Highly Efficient Electrophosphorescent Devices. *Adv. Mater.* **2011**, *23*, 3876−3895.

(23) Sudhakar, M.; Djurovich, P. I.; Hogen-Esch, T. E.; Thompson, M. E. Phosphorescence Quenching by Conjugated Polymers. *J. Am. Chem. Soc.* **2003**, *125*, 7796−7797.

(24) Ge, Z.; Hayakawa, T.; Ando, S.; Ueda, M.; Akiike, T.; Miyamoto, H.; Kajita, T.; Kakimoto, M. Spin-Coated Highly Efficient Phosphorescent Organic Light-Emitting Diodes Based on Bipolar Triphenylamine-Benzimidazole Derivatives. *Adv. Funct. Mater.* **2008**, *18*, 584−590.

(25) Arias, A. C.; MacKenzie, J. D.; McCulloch, I.; Rivnay, J.; Salleo, A. Materials and Applications for Large Area Electronics: Solution-Based Approaches. *Chem. Rev.* **2010**, *110*, 3−24.

(26) Cai, M.; Xiao, T.; Hellerich, E.; Chen, Y.; Shinar, R.; Shinar, J. High-Efficiency Solution-Processed Small Molecule Electrophosphorescent Organic Light-Emitting Diodes. *Adv. Mater.* **2011**, *23*, 3590−3596.

(27) Choi, M. C.; Kim, Y.; Ha, C. S. Polymers for Flexible Displays: From Material Selection to Device Applications. *Prog. Polym. Sci.* **2008**, *33*, 581−630.

(28) Cho, S. H.; Yoon, J.; Chang, S. Intramolecular Oxidative C-N Bond Formation for The Synthesis of Carbazoles: Comparison of Reactivity Between The Copper-Catalyzed and Metal-Free Conditions. *J. Am. Chem. Soc.* **2011**, *133*, 5996−6005.

(29) Kim, D.; Coropceanu, V.; Bredas, J. L. Design of Efficient Ambipolar Host Materials for Organic Blue Electrophosphorescence: Theoretical Characterization of Hosts Based on Carbazole Derivatives. *J. Am. Chem. Soc.* **2011**, *133*, 17895−17900.

(30) Shao, S.; Ding, J.; Ye, T.; Xie, Z.; Wang, L.; Jing, X.; Wang, F. A Novel, Bipolar Polymeric Host for Highly Efficient Blue Electrophosphorescence: A Non-Conjugated Poly(aryl ether) Containing Triphenylphosphine Oxide Units in The Electron-Transporting Main Chain and Carbazole Units in Hole-Transporting Side Chains. *Adv. Mater.* **2011**, *23*, 3570−3574.

DOI: 10.1021/acsami.5b04112
ACS Appl. Mater. Interfaces 2015, 7, 17802−17810

(31) Hudson, Z. M.; Wang, Z.; Helander, M. G.; Lu, Z. H.; Wang, S. N-Heterocyclic Carbazole-Based Hosts for Simplified Single-Layer Phosphorescent OLEDs with High Efficiencies. *Adv. Mater.* **2012**, *24*, 2922−2928.
(32) Wang, X.; Wang, S.; Ma, Z.; Ding, J.; Wang, L.; Jing, X.; Wang, F. Solution-Processible 2, 2′-Dimethyl-biphenyl Cored Carbazole Dendrimers as Universal Hosts for Efficient Blue, Green, and Red Phosphorescent OLEDs. *Adv. Funct. Mater.* **2014**, *24*, 3413−3421.
(33) Xia, D.; Wang, B.; Chen, B.; Wang, S.; Zhang, B.; Ding, J.; Wang, L.; Jing, X.; Wang, F. Self-Host Blue-Emitting Iridium Dendrimer with Carbazole Dendrons: Nondoped Phosphorescent Organic Light-Emitting Diodes. *Angew. Chem., Int. Ed.* **2014**, *53*, 1048−1052.
(34) Jou, J. H.; Chen, C. C.; Wang, W. B.; Hsu, M. F.; Wang, C. J.; Chen, C. T.; Wu, M. F.; Chen, H. Y.; Shyue, J. J.; Chin, C. L. A New Door For Molecular-Based Organic Light-Emitting Diodes. *Proc. SPIE* **2008**, *7051*, 70510P−70510P-10.
(35) Tsuboi, T.; Liu, S. W.; Wu, M. F.; Chen, C. T. Spectroscopic and Electrical Characteristics of Highly Efficient Tetraphenylsilane-Carbazole Organic Compound as Host Material for Blue Organic Light Emitting Diodes. *Org. Electron.* **2009**, *10*, 1372−1377.
(36) Su, S. J.; Takahashi, Y.; Chiba, T.; Takeda, T.; Kido, J. Structure−Property Relationship of Pyridine-Containing Triphenyl Benzene Electron-Transport Materials for Highly Efficient Blue Phosphorescent OLEDs. *Adv. Funct. Mater.* **2009**, *19*, 1260−1267.
(37) Sun, D.; Yang, Z.; Ren, Z.; Li, H.; Bryce, M. R.; Ma, D.; Yan, S. Oligosiloxane Functionalized with Pendant (1, 3-Bis (9-carbazolyl) benzene) (mCP) for Solution-Processed Organic Electronics. *Chem. - Eur. J.* **2014**, *20*, 16233−16241.
(38) Sun, D.; Zhou, X.; Li, H.; Sun, X.; Zheng, Y.; Ren, Z.; Ma, D.; Bryce, M. R.; Yan, S. A Versatile Hybrid Polyphenylsilane Host for Highly Efficient Solution-Processed Blue and Deep Blue Electrophosphorescence. *J. Mater. Chem. C* **2014**, *2*, 8277−8284.
(39) Sun, D.; Zhou, X.; Liu, J.; Sun, X.; Li, H.; Ren, Z.; Ma, D.; Bryce, M. R.; Yan, S. Solution-Processed Blue/Deep Blue and White Phosphorescent Organic Light-Emitting Diodes (PhOLEDs) Hosted by a Polysiloxane Derivative with Pendant mCP (1, 3-bis (9-carbazolyl) benzene). *ACS Appl. Mater. Interfaces* **2015**, 150204094434000.

DOI: 10.1021/acsami.5b04112
ACS Appl. Mater. Interfaces 2015, 7, 17802−17810